Increased Rates of Genomic Deletions Generated by Mutations in the Yeast Gene Encoding DNA Polymerase δ or by Decreases in the Cellular Levels of DNA Polymerase δ

ROBERT J. KOKOSKA, LELA STEFANOVIC, JEREMY DeMAI, AND THOMAS D. PETES*

Department of Biology, Curriculum in Genetics and Molecular Biology, University of North Carolina, Chapel Hill, North Carolina 27599-3280

In *Saccharomyces cerevisiae*, *POL3* encodes the catalytic subunit of DNA polymerase δ. While yeast *POL3* mutant strains that lack the proofreading exonuclease activity of the polymerase have a strong mutator phenotype, little is known regarding the role of other Pol3p domains in mutation avoidance. We identified a number of *pol3* mutations in regions outside of the exonuclease domain that have a mutator phenotype, substantially elevating the frequency of deletions. These deletions appear to reflect an increased frequency of DNA polymerase slippage. In addition, we demonstrate that reduction in the level of wild-type DNA polymerase results in a similar mutator phenotype. Lowered levels of DNA polymerase also result in increased sensitivity to the DNA-damaging agent methyl methane sulfonate. We conclude that both the quantity and the quality of DNA polymerase δ is important in ensuring genome stability.

The low mutation rate observed in wild-type cells reflects both the accuracy of DNA polymerases and the existence of DNA repair systems that remove misincorporated bases. Mutations affecting components of either of these systems can result in a mutator phenotype, a global elevation in mutation frequencies throughout the genome (27). In the yeast *Saccharomyces cerevisiae*, a mutator phenotype has been associated with certain mutations of *POL3* and *POL2*, encoding the replicative DNA polymerases δ and ε, respectively (12, 22, 37, 55); these alleles can reside in either a DNA-proofreading exonuclease domain of *POL3* (Exo I domain [Fig. 1]) or near domains required for nucleotide binding (domains II and VI). Certain mutant substitutions of *POL30*, encoding the DNA polymerase processivity factor PCNA, also have a strong mutator phenotype (8, 20, 23, 56). In addition, null mutations of *RAD27* (encoding an Okazaki fragment-processing enzyme) or certain alleles of *RPA1* (encoding the large subunit of a single-stranded DNA binding protein) substantially elevate mutation rates (7, 19, 22, 54). A number of mutants in *Schizosaccharomyces pombe*, including those affecting DNA polymerases α and δ and DNA ligase, also exhibit increased rates of mutation (33).

In addition to mutations affecting DNA replication genes, mutations of the DNA mismatch repair genes have a mutator phenotype. Most mismatch repair in yeast involves two complexes, although other complexes have minor roles (24). Base-base mismatches are corrected by a heterotetramer involving Msh2p, Msh6p, Pms1p, and Mlh1p. Small DNA loops, resulting from DNA polymerase slippage events on simple repetitive DNA sequences (microsatellites) (Fig. 2A), are repaired by a complex that includes Msh2p, Msh3p, Pms1p, and Mlh1p. Failure to repair base-base mismatches results in an elevated frequency of single-base-pair substitutions, whereas failure to repair DNA loops results in an elevated frequency of deletions or insertions (47). Genetic and biochemical data indicate that the Msh2p-Msh3p Pms1p-Mlh1p complex can correct DNA loops up to 14 bases in size but is incapable of correcting loops that are 16 bases or greater (13, 35, 48, 49, 51, 52).

Although some mutators affect only DNA replication or DNA mismatch repair, other mutators are likely to affect both processes. For example, some *pol30* alleles both reduce the efficiency of DNA mismatch repair and increase the rate of DNA polymerase slippage (8, 20, 56).

Mutators differ in two ways: the degree to which they elevate mutation rates and the types of mutations that are elevated. For purposes of this discussion, we will classify mutations as single-base-pair substitutions, frameshifts (additions or deletions of repeat units to a repetitive tract of DNA), or additions and deletions involving nonrepetitive DNA sequences. Mutant substitutions affecting the proofreading exonuclease domain of DNA polymerase (*pol3-01* and *pol2-4*) greatly increase the frequency of base pair substitutions but have a modest effect on the stability of long microsatellites (37, 51). A different allele of *POL3* (*pol3-t*) and several of the *POL30* and *RPA1* alleles greatly increase the rate of deletions involving nonrepetitive DNA sequences (7, 8, 12), whereas mutations in *RAD27* increase the frequency of duplications (19, 22, 54). Mutations that affect DNA mismatch repair enzymes elevate both single-base-pair substitutions and frameshifts, but the elevation observed for frameshifts is much greater (47).

Since only two mutator alleles of *POL3* have been described, we decided to do a genetic screen for new mutator alleles of this gene. Following random mutagenesis of the entire *POL3* gene, we isolated and characterized three new missense mutants. We unexpectedly also isolated a number of other mutator alleles that were nonsense mutations within *POL3*. As discussed below, our analysis of these mutants and strains in which the level of DNA polymerase δ was reduced demonstrated a novel mechanism for producing a mutator phenotype.

MATERIALS AND METHODS

Media. Standard enriched (YPD) or minimal (SD) growth medium for yeast was utilized (46). Media for the growth of strains containing *POL3* under the control of the *GAL1/10* promoter consisted of 1% Bacto Yeast Extract, 2% Bacto Peptone, 3% raffinose (YPR), and various concentrations of galactose as indicated.

* Corresponding author. Mailing address: Department of Biology and Curriculum in Genetics and Molecular Biology, University of North Carolina, Chapel Hill, NC 27599-3280. Phone: (919) 962-1445. Fax: (919) 962-8472. E-mail: tompetes@email.unc.edu.
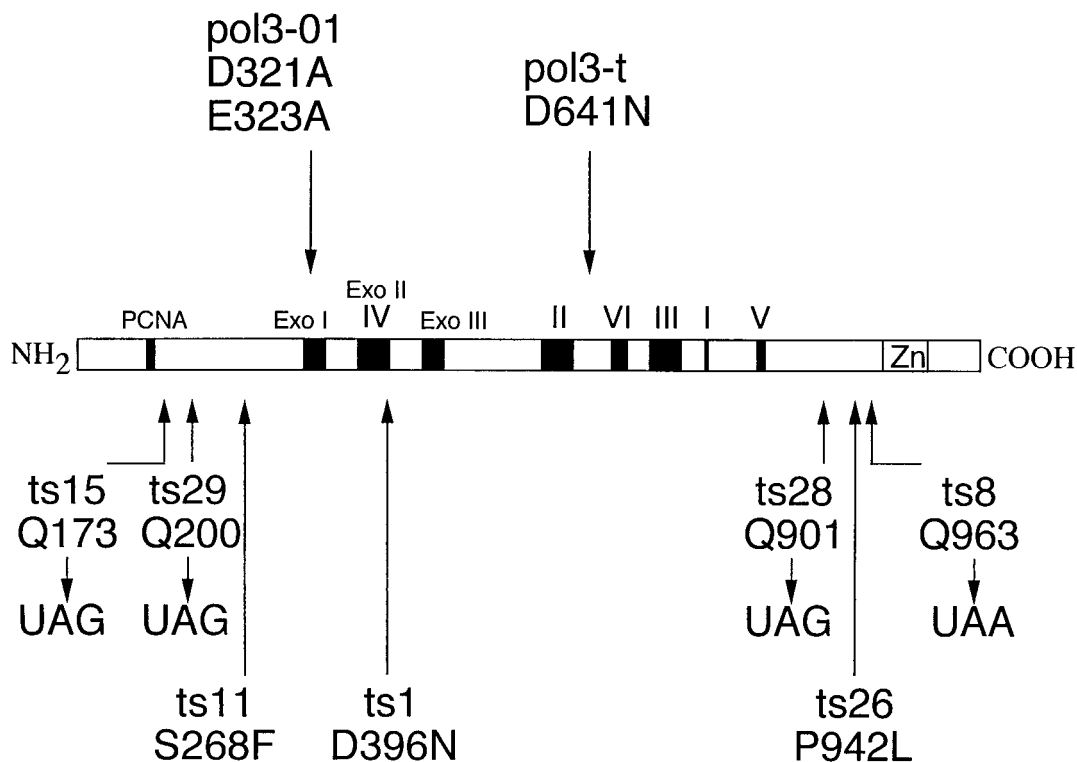
FIG. 1. Arrangement of conserved domains in yeast Pol3p (16) and locations of amino acid alterations in *POL3* mutants. *POL3* encodes a polypeptide of 124 kDa (1,097 amino acids). The coding sequence includes three regions corresponding to the exonuclease proofreading active site (Exo I, II, and III; Exo II is contained within domain IV). Other conserved domains include a catalytic center (domain I), regions thought to be involved in nucleotide binding (domains II, III, and V), and a putative zinc finger DNA binding domain (Zn) (58). A putative PCNA-interacting domain (PCNA) is located in the N-terminal region of the protein (61). The locations of the mutator alleles *pol3-01* (37) and *pol3-t* (12) are shown in the upper half of the diagram. The amino acid substitutions of the unique *POL3* missense and nonsense alleles characterized in this paper are indicated in the lower half of the diagram.

Yeast strains and plasmids. The yeast strains used in this study are listed in Table 1. All of the strains are isogenic with AMY125 (α *ade5-1 leu2-3 trp1-289 ura3-52 his7-2* [51]) except for changes introduced by transformation. EAS63a (provided by E. Sia) was a derivative of MS71 in which the mating type was switched, the *ade5-1* mutation was reverted, and a poly(GT) tract 29 bp in length was inserted into the *ADE2* gene (*ade2-100*). RJK48 is a *leu2* derivative of EAS63a constructed by targeted disruption of the *LEU2* gene with *Bgl*II-treated pNKY85 (1).

The plasmid pBL304 contains the wild-type *POL3* gene cloned into YCp50. The plasmid pBK100, in which the *URA3* of pBL304 was replaced with *LEU2*, was generated in vivo by transforming the strain RJK67-5 (RJK48 plus pBL304) with a PCR fragment containing the *LEU2* gene flanked by 40 bp of *URA3* homology; this fragment was generated by PCR using *Sal*I/*Hin*dIII-digested pRS315 (*LEU2*) as a template and the primers 5'-AACCCTTGGCAGAACAT ATCCATCGCGTCCGCCATCTCCAtcaattgtcctgtacttcc and 5'-GTGATTCAT TCTGCTAACCAGTAAGGCAACCCCCGCCAGCCtaaggccgtttctgacaga (the bases in lowercase indicate *LEU2*-specific sequences).

To delete the chromosomal copy of *POL3*, we transformed RJK67-5 with a PCR-generated fragment in which the *kanMX* gene is flanked by DNA sequences derived from the regions upstream and downstream of *POL3*. The oligonucleotides used for the amplification were 5'-TTGCTATTAAGCATTAATCTTTAT ACATATACGCACAGCAcgtacgctgcaggtcgac and (downstream) 5'-CCTTTCT TAATCCTAATATGATGTGCCACCCTATCGTTTTatcgatgaattcgagctcg (the lowercase letters correspond to *kanMX* sequences); the substrate for the amplification reaction was a plasmid containing Tn*903* (57). The resulting strain was RJK122-3. Strains similar to RJK122-3 with plasmid-borne copies of *POL3* or mutant *pol3* genes were isolated by the plasmid shuffle technique described below. To create strains bearing *rad52Δ* and/or *msh3Δ* in combination with the plasmid-borne *POL3* genes, we formed diploids by crossing appropriate haploid strains, sporulated the diploids, and identified spore colonies that contained the desired genotypes.

The strain RJK341 contains a version of *POL3* in which an epitope (3 × HA) is inserted at the N terminus of *POL3* and the promoter is replaced with the *GAL1/10* promoter; a *kanMX* cassette is immediately upstream of the *GAL1/10* promoter. This strain was constructed by transforming MS71 with a DNA fragment generated by PCR amplification of pFA6a-kanMX6-PGAL1-3HA as a template (34) using the primers 5'-TATTGAGCACTTGCTATTAAGCATTA ATCTTTATACATATgaattcgagctcgtttaaac and 5'-TCTTCACATCAACCATG

GGAAGGGATCTTTTTTCACTCATgcactgagcagcgtaatctg. The uppercase sequences correspond to nucleotides −49 to −10 and nucleotides +40 to +1 relative to the *POL3*-initiating AUG. The construction replaces the 9 nucleotides just upstream of the *POL3*-initiating AUG with the *kanMX* cassette, the *GAL1/ 10* promoter, and the 3×HA tag. The epitope tag is present with its own initiating codon downstream of the *GAL1/10* promoter and is in frame and directly upstream of the entire *POL3* coding sequence.

The strain JED213-30 has a 3×HA epitope tag inserted into a wild-type *POL3* gene. This strain was constructed by transforming the strain MS71-*pol3-t* (which has a temperature-sensitive *pol3* allele) with a PCR fragment designed to simultaneously revert the *pol3-t* allele and insert the 3×HA epitope tag at the beginning of the *POL3* coding sequence. This PCR fragment was generated using genomic DNA from strain RJK341 as a template with the following primers: upstream, 5'-AAATAGATATTGAGCACTTGCTATTAAGCATTAATCTTT ATACATATACGCACAGCAatgtctttaattaacatcttt, and downstream, 5'-CAAT AGAAACCAAGGAACAGGAATC. The sequence shown in uppercase on the first primer corresponds to nucleotides −57 to −1 relative to the *POL3* start codon, and the lowercase letters correspond to the first 21 nucleotides of the 3×HA epitope tag coding sequence. The downstream primer consists of nucleotides 2545 to 2521 of *POL3*. Transformants were selected by growth at 37°C.

PEP4 was deleted by replacing it with *URA3*. The DNA fragment used for this replacement was generated by PCR using pRS306 (*URA3*) as the template and the following two primers (*PEP4* sequences are capitalized): upstream, 5'-GTA TTTAATCCAAATAAAATTCAAACAAAAACCAAAACTAACcgctttcaattca attc, and downstream, 5'-GCAGAAAAGGATAGGGCGGAGAAGTAAGAA AAGTTTAGCcagggtaataactgatataa.

To evaluate the effects of various mutations on dinucleotide repeat instability, we transformed appropriate strains with pSH44 [*CEN TRP1*] (15). This plasmid contains a 33-bp poly(GT) tract inserted in frame within the *URA3* coding sequence.

***POL3* mutagenesis and mutant isolation.** The *POL3* gene was randomly mutagenized by treating pBK100 with hydroxylamine (50). Following mutagenesis of pBK100, *POL3* mutants were isolated by the plasmid shuffle technique (50). Yeast strain RJK122-3 was transformed with 1 μg of the mutagenized pBK100, plated on solid minimal medium lacking leucine, and incubated at 22°C for 5 days. The Leu⁺ colonies were replica plated onto two plates containing minimal medium lacking leucine and containing 5-fluoroorotate (5-FOA). This selection (4) allows for growth of cells that have lost the pBL304 plasmid and retained the
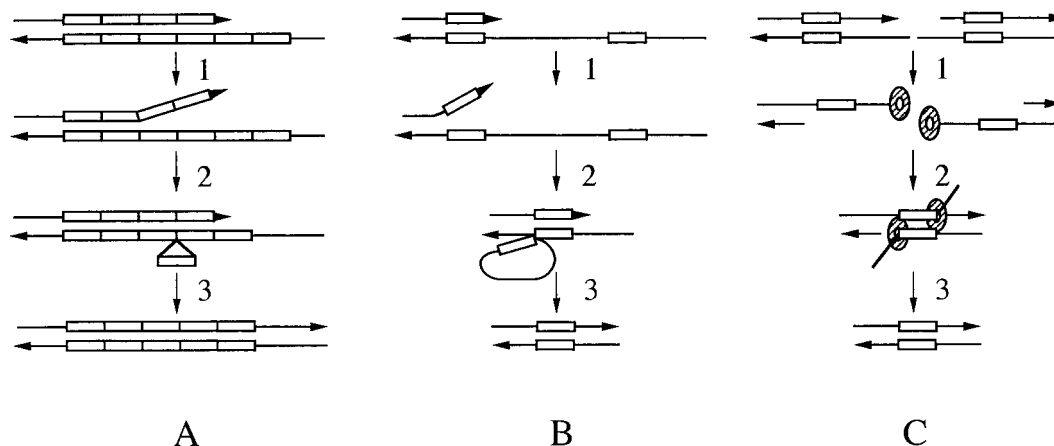
FIG. 2. Deletions involving repetitive DNA elements. (A) Deletions generated within simple repetitive tracts by DNA polymerase slippage. The top strand of each pair represents the primer strand, and the bottom strand represents the complementary template. The horizontal arrows indicate the 3′ ends of the template strands, and the triangles show the 3′ ends of the primer strands. The rectangles illustrate the repeat units within the tracts. As replication proceeds through this repeat region, polymerase dissociation can allow strand separation (step 1) followed by misaligned reannealing (step 2), resulting in a loop of unpaired bases on the template strand consisting of an integral number of repeat units. Uncorrected loops would result in a deletion of a repeat unit(s) following the next round of replication (step 3). Insertions can also be generated if the unrepaired loop appears on the primer strand. (B) Deletions between nontandem direct repeats generated by DNA polymerase slippage. The rectangles represent two small repeats of identical sequence. Following replication of one of these units, polymerase dissociation and strand separation (step 1) can be followed by reannealing of the 3′ end of the primer to the complementary region of the downstream repeat unit. The resulting intermediate contains a loop on the template strand consisting of one of the repeat units and the unique sequence between the repeats (step 2). Failure to correct this loop results in a large deletion (step 3). (C) Deletions between nontandem direct repeats generated by SSA (40). The bottom and top strand of each structure represents the template strand and two adjacent Okazaki fragments, respectively, with DNA synthesis proceeding from left to right. The rectangles represent two small units of identical sequence. Prolonged exposure of single-stranded DNA on the template strand can result in cleavage within this region, forming a double-strand break. The 5′ ends present at the break can be resected by an exonuclease activity (step 1). Exposure of the complementary nontandem-repeat units allow these short tracts to anneal (step 2). This annealing may be promoted by Rad52p (shown as shaded circles). Processing of the 3′ noncomplementary tails (step 3) results in a deletion.

mutagenized plasmid. Isolates containing potential temperature-sensitive lethal *POL3* mutants were distinguished by growth on 5-FOA medium at 22°C and loss of growth on this medium at 37°C.

Assays for cell viability and sensitivity to DNA damage. For the experiments that tested for cell viability upon loss of [*PSI*⁺], strains were grown at 22°C on solid YPD medium to single colonies. The colonies were replica plated onto YPD medium with or without 5 mM guanidine hydrochloride (GuHCl) and grown overnight at 22°C. The replica plating was repeated twice more onto identical media. To test the damage sensitivity of the temperature-sensitive *POL3* mutants, we pregrew yeast strains on solid YPD medium for 2 days at 22°C. For the similar experiments that utilized the strain bearing the *GAL1-POL3* construct, strains were pregrown on solid YPR medium containing 0.05% galactose for 2 days at 30°C. Fivefold serial dilutions of each strain were spotted onto appropriate media. To test for UV sensitivity, we treated patches of cells of various serial dilutions with UV light from a germicidal lamp. MMS (methyl methane sulfonate) sensitivity was examined by spotting serial dilutions on appropriate solid medium containing 0.025% MMS. All plates were incubated for 3 to 4 days in the dark at 30°C.

Determination of spontaneous mutation rates and mutational spectra. The forward mutation rate at the *CAN1* locus was determined by standard methods (48), using at least 12 independent cultures for each rate estimate. Rates were calculated from the frequencies of canavanine-resistant mutants by using the method of the median (28). For strains bearing the *GAL1/10* promoter upstream of *POL3*, the cells were pregrown in YPR medium containing appropriate concentrations of galactose.

The mutant substitutions in *CAN1* were analyzed by PCR amplification of the 1.8-kb *CAN1* gene. Primers located at three positions within the gene were used in the sequence analysis. For some experiments, the 1.8-kb *CAN1* gene was treated with *Ssp*I and the resulting fragments (with sizes of 515, 652, and 718 bp) were examined by electrophoresis using 2% Metaphor (FMC Corp.) agarose gels; this method can detect deletions as small as 8 bp. The extents of deletions that removed one or both ends of *CAN1* were determined using 14 primer pairs to amplify sequences centromere-distal to *CAN1* (7). The sequence of deletions followed by telomeric additions was determined by a PCR procedure utilizing a series of degenerate primers (7).

Analysis of plasmid-borne simple-repeat instability. Yeast strains were transformed with pSH44 to determine the rate of instability within a 33-bp poly(GT) tract by methods described previously (15). Alterations within the repetitive tract were determined by PCR amplification of the repetitive region and analysis by gel electrophoresis as described previously (48).

Western blot analysis. Liquid cultures for RJK368-4 were grown in YPR medium containing various concentrations of galactose and those for RJK366-5 and RJK394 were grown in YPD medium to mid-log phase. Protein extracts from spheroplasts of these strains were prepared as described previously (2). Proteins were fractionated on a sodium dodecyl sulfate–7.5% polyacrylamide gel, trans-

ferred to nitrocellulose, and blocked by standard procedures (43). Membranes were probed with mouse antihemagglutinin (anti-HA) monoclonal antibody (clone 12CA5) (Boehringer Mannheim). Detection of antibody binding was performed using horseradish peroxidase-linked anti-mouse immunoglobulin G (Amersham). Quantitation of protein bands was performed on a scanning densitometer (Molecular Dynamics). Quantitation was based on the intensity of a band specific to Pol3p normalized by the intensity of a band representing a protein that is nonspecifically recognized by the HA antibody.

Statistical methods. Calculation of 95% confidence intervals was done as described previously (22). Fisher exact tests were performed using the InStat version 1.12 program.

RESULTS

Isolation and phenotypes of yeast *POL3* missense mutants. In order to identify new mutator alleles of DNA polymerase δ, we isolated mutants of the yeast *POL3* gene by the plasmid shuffle technique (50). The plasmid pBK100 (YCp *POL3 LEU2*) was randomly mutagenized by treating the plasmid DNA with hydroxylamine. This mutagenized plasmid was transformed into a yeast strain containing pBL304 (YCp *POL3 URA3*) and a deletion of the *POL3* chromosomal locus. Cells derived from each transformant that lost pBL304 were detected on medium containing 5-FOA, which selects against Ura⁺ cells (4). In order to increase the probability of identifying strains with a mutagenized *POL3* gene, we screened the transformants containing mutagenized pBK100 (7,500 strains examined) for temperature sensitivity (loss of growth at 37°C) on minimal growth medium containing 5-FOA; *POL3* is an essential gene in yeast, and temperature-sensitive alleles of *POL3* were previously isolated (14). Ten independent strains with a temperature-sensitive *pol3* mutation were identified. DNA sequence analysis of these mutant alleles showed that four (*pol3-ts1*, *pol3-ts11*, *pol3-ts18*, and *pol3-ts26*), representing three different alterations (*pol3-ts1* is equivalent to *pol3-ts18*), contained single missense mutations within the *POL3* gene. The positions and amino acid alterations of these mutations are shown in Fig. 1.

TABLE 1. Yeast strains

Strain	Relevant genotype[a]	Source or construction
MS71	*LEU2*	52
EAS63a	**a** *ade2-100 ADE5 LEU2*	E. A. Sia
RJK48	**a** *ade2-100 ADE5*	Described in Materials and Methods
HM6	*LEU2 rad52Δ::hisG-URA3-hisG*	H. Moore
GCY140	*LEU2 msh3Δ*	52
RJK341	*LEU2 kanMX-GAL1-(3×HA)-POL3*	Described in Materials and Methods
RJK368-4	*LEU2 kanMX-GAL1-(3×HA)-POL3 pep4::URA3*	Described in Materials and Methods
MS71-*pol3-t*	*LEU2 pol3-t*	22
JED213-30	*LEU2 (3×HA)-POL3*	Described in Materials and Methods
RJK394	*LEU2 (3×HA)-POL3 pep4::URA3*	Described in Materials and Methods
RJK366-5	*LEU2 pep4::URA3*	Described in Materials and Methods
RJK370	**a** *rad52Δ::hisG-URA3-hisG*	Spore from RJK364[b]
RJK396	**a** *LEU2*	Spore from RJK372[b]
RJK397	*rad52Δ::hisG-URA3-hisG*	Spore from RJK372[b]
RJK398	*kanMX-GAL1-(3×HA)-POL3*	Spore from RJK372[b]
RJK399	**a** *LEU2 rad52Δ::hisG-URA3-hisG kanMX-GAL1-(3×HA)-POL3*	Spore from RJK372[b]
LS31	*rev3Δ::kanMX*	J. Gerton
EAS102	*LEU2 rad1Δ*	E. A. Sia
RJK67-5	**a** *ade2-100 ADE5* + pBL304[*CEN4/URA3/POL3*]	RJK48 transformed with pBL304
RJK78-3	**a** *ade2-100 ADE5* + pBK100 [*CEN4/LEU2/POL3*]	Described in Materials and Methods
RJK122-3	**a** *ade2-100 ADE5 pol3::kanMX* + pBL304	Described in Materials and Methods
RJK160-1	**a** *ade2-100 ADE5 pol3::kanMX* + pBK100	Plasmid shuffle of RJK122-3[c]
RJK158-3	**a** *ade2-100 ADE5 pol3::kanMX* + pBK101 [*CEN4/LEU2/pol3-ts1*]	Plasmid shuffle of RJK122-3[c]
RJK185-1	**a** *ade2-100 ADE5 pol3::kanMX* + pBK102 [*CEN4/LEU2/pol3-ts8*]	Plasmid shuffle of RJK122-3[c]
RJK187-1	**a** *ade2-100 ADE5 pol3::kanMX* + pBK103 [*CEN4/LEU2/pol3-ts11*]	Plasmid shuffle of RJK122-3[c]
RJK218-2	**a** *ade2-100 ADE5 pol3::kanMX* + pBK104 [*CEN4/LEU2/pol3-ts15*]	Plasmid shuffle of RJK122-3[c]
RJK223-1	**a** *ade2-100 ADE5 pol3::kanMX* + pBK105 [*CEN4/LEU2/pol3-ts26*]	Plasmid shuffle of RJK122-3[c]
RJK286-1	**a** *ade2-100 ADE5 pol3::kanMX* + pBK106 [*CEN4/LEU2/pol3-ts28*]	Plasmid shuffle of RJK122-3[c]
RJK287-1	**a** *ade2-100 ADE5 pol3::kanMX* + pBK107 [*CEN4/LEU2/pol3-ts29*]	Plasmid shuffle of RJK122-3[c]
RJK288	**a** *ade2-100 ADE5 pol3::kanMX rad52Δ::hisG-URA3-hisG* + pBK101	Spore from RJK272[b]
RJK334	**a** *ade2-100 ADE5 pol3::kanMX rad52Δ::hisG-URA3-hisG* + pBK100	Spore from RJK310[b]
RJK335	**a** *ade2-100 ADE5 pol3::kanMX rad52Δ::hisG-URA3-hisG* + pBK100	Spore from RJK310[b]
RJK357	**a** *ade2-100 ADE5 pol3::kanMX msh3Δ* + pBK100	Spore from RJK344[b]
RJK358	**a** *ade2-100 ADE5 pol3::kanMX msh3Δ* + pBK101	Spore from RJK345[b]
RJK363	**a** *ade2-100 ADE5 pol3::kanMX msh3Δ rad52Δ::hisG-URA3-hisG* + pBK101	Spore from RJK345[b]
RJK381	**a** *ade2-100 ADE5 pol3::kanMX msh3Δ rad52Δ::hisG-URA3-hisG* + pBK101	Spore from RJK373[b]
RJK379	**a** *ade2-100 ADE5 pol3::kanMX msh3Δ rad52Δ::hisG* + pBK101	5-FOA[r] isolate of RJK363
RJK242-1	**a** *ade2-100 ADE5 pol3::kanMX* + pBK100 + pSH44	RJK160-1 transformed with pSH44
RJK166-4	**a** *ade2-100 ADE5 pol3::kanMX* + pBK101 + pSH44	RJK158-3 transformed with pSH44
RJK202-3	**a** *ade2-100 ADE5 pol3::kanMX* + pBK103 + pSH44	RJK187-1 transformed with pSH44
RJK232-5	**a** *ade2-100 ADE5 pol3::kanMX* + pBK105 + pSH44	RJK223-1 transformed with pSH44
LS38-1	**a** *ade2-100 ADE5 pol3::kanMX msh3Δ* + pBK100 + pSH44	RJK357 transformed with pSH44
LS40-1	**a** *ade2-100 ADE5 pol3::kanMX msh3Δ* + pBK101 + pSH44	RJK358 transformed with pSH44
RJK380-1	**a** *ade2-100 ADE5 pol3::kanMX msh3Δ rad52Δ::hisG* + pBK101 + pSH44	RJK379 transformed with pSH44

[a] All strains are isogenic with AMY125 (α *trp1-289 his7-2 ura3-52 leu2-3 ade5-1* [51]) except for the changes introduced by transformation. Only alterations from the AMY125 genotype are shown.

[b] Diploids referred to were constructed by the following crosses: RJK310 (RJK160-1 × HM6), RJK344 (RJK160-1 × GCY140), RJK345 (RJK288 × GCY140), RJK272 (RJK158-3 × HM6), RJK373 (RJK358 × HM6), RJK364 (LS31 × RJK288), and RJK372 (RJK341 × RJK370).

[c] These strains were generated by transforming RJK122-3 with mutagenized pBK100, followed by screening for derivatives of the transformed strain that lost the pBL304 plasmid.

These *POL3* missense mutants were examined for abnormal cell growth at the semipermissive temperature (30°C) and were screened for sensitivity to DNA damage. Many of the mutant cells had buds approximately the same size as the mother cell. The percentages of cells with this morphology at 30°C for the wild type, *pol3-ts1*, *pol3-ts11*, and *pol3-ts26* were 7, 39, 18, and 63%, respectively (500 cells were counted). After the incubation of cells at 37°C for 20 h, the percentages of cells with this morphology for the wild-type, *pol3-ts1*, *pol3-ts11*, and *pol3-ts26* were 6, 98, 95, and 95%, respectively (500 cells were counted). The accumulation of large-budded cells at 37°C suggests that the growth defect associated with these mutant strains is due to a defect in DNA replication that does not allow for efficient completion of S phase, since a similar position of cell cycle arrest is observed for other types of mutations affecting DNA synthesis (29). Each *POL3* mutant also exhibited moderate to high sensitivity to MMS but no sensitivity to UV radiation, suggesting that the mutant polymerases confer specific defects in the repair of damaged DNA. An example of these phenotypes for the *pol3-ts1* mutants is shown in Fig. 3. Strains with *rad1Δ* (conferring sensitivity to UV) or *rad52Δ* (conferring sensitivity to MMS) mutations are shown as controls.

POL3 missense mutants exhibit mutator phenotypes and dissimilarities in mutational spectra. To determine if the strains bearing the *POL3* missense mutations conferred a mutator phenotype, we assayed for the forward mutation rate at the *CAN1* locus in vivo. Wild-type cells are sensitive to the arginine analog canavanine, and any mutation that inactivates the arginine permease encoded by *CAN1* results in canavanine resistance. We found that strains bearing any of the three *POL3* alleles exhibit four- to sixfold-elevated rates of mutation at *CAN1* (Table 2).
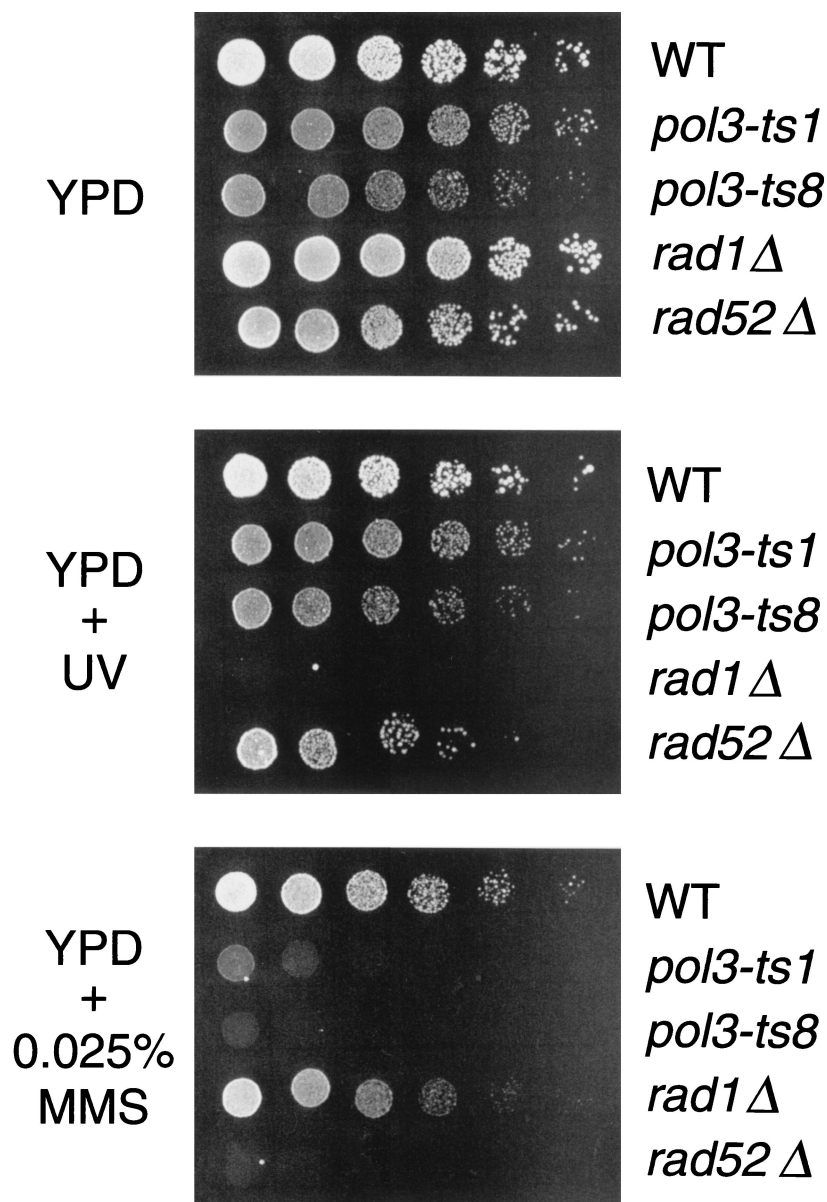
FIG. 3. Sensitivity of *pol3* mutant strains to DNA damage. Fivefold serial dilutions of each strain were spotted onto YPD plates in the presence of MMS or subjected to UV irradiation. The strains examined were RJK160-1 (wild-type [WT]; top rows), RJK158-3 (missense mutant *pol3-ts1*; second rows), RJK185-1 (nonsense mutant *pol3-ts8*, third rows), EAS102 (*rad1Δ*; fourth rows), and HM6 (*rad52Δ*, bottom rows). The results were similar for all *POL3* missense and nonsense mutants identified in this study. The *rad1Δ* strain was used as a control for UV sensitivity, and the *rad52Δ* strain was the control for MMS sensitivity.

Although all of these strains are mutators, they do not display the same spectrum of mutations. The mutational spectrum for each strain was determined by sequencing the *CAN1* gene from approximately 20 independent canavanine-resistant (Can^r) isolates. As shown in Table 3, over one-half of the mutations generated in the *pol3-ts1* and *-ts11* strains were deletions larger than a few base pairs. The deletions within *CAN1* in the *pol3-ts1* strain ranged from 16 to 336 bp in length, while the *pol3-ts11* mutation resulted in deletions of 16 to 864 bp. One distinguishing characteristic of each of the sequenced *CAN1* deletions is the presence of an imperfect direct repeat flanking each deletion. These repeat motifs range from 5 to 11 bp (Table 4); with one exception, each pair of flanking repeats has a perfect match of at least 75% of the bases. These types of deletions have been previously observed in strains bearing

the *rfa1-t29* allele of *S. cerevisiae* (7) and several *pol3* alleles of *S. pombe* (33). In addition, one canavanine-resistant isolate in the *pol3-ts11* strain exhibited a complete deletion of approximately 35,000 bp of one end of chromosome V (including the entire *CAN1* gene) and the addition of a telomeric sequence (repeats of TG$_{1-3}$); the breakpoint of this deletion mutation occurred in a GT-rich region of the chromosome (Table 3). Telomeric additions have previously been observed in other strains with mutations affecting DNA repair or replication (6, 7) or associated with repair of an HO-induced DNA break (25). Only 20% of the mutations generated within these *pol3* strains are base substitutions. Since 55% of the sequenced mutations in an isogenic wild-type strain are substitutions, it appears that *pol3-ts1* and *-ts11* have a small (or no) effect on the accumulation of this class of mutation.

TABLE 2. Forward mutation rates at *CAN1* in strains with *POL3* missense mutations and/or mutations affecting DNA repair or recombination

Strain genotype[a]	Rate of canavanine resistance (10^{-7} per cell division)[b]	95% Confidence interval (10^{-7} per cell division)
WT	2.4 (1)	2.3–2.9
pol3-ts1	14 (6)	10–18
pol3-ts11	10 (4)	9.4–13
pol3-ts26	9.7 (4)	8.5–11
msh3	2.5 (1)	2.1–3.2
rad52 isolate 1	27 (11)	24–33
rad52 isolate 2	29 (12)	25–40
pol3-ts1 msh3	47 (20)	42–62
pol3-ts1 rad52	63 (26)	48–77
pol3-ts1 msh3 rad52 isolate 1	50 (21)	45–75
pol3-ts1 msh3 rad52 isolate 2	42 (18)	22–48

[a] Strain names are as follows: RJK160-1 (wild type [WT]), RJK158-3 (*pol3-ts1*), RJK187-1 (*pol3-ts11*), RJK223-1 (*pol3-ts26*), RJK357 (*msh3*), RJK334 (*rad52* isolate 1), RJK335 (*rad52* isolate 2), RJK358 (*pol3-ts1 msh3*), RJK288 (*pol3-ts1 rad52*), RJK363 (*pol3-ts1 msh3 rad52* isolate 1), and RJK381 (*pol3-ts1 msh3 rad52* isolate 2).
[b] Numbers given in parentheses are fold increase over wild type.

In contrast to the results obtained with *pol3-ts1* and *-ts11*, 70% of all Can[r] isolates derived from the *pol3-ts26* allele are single-base substitutions. Fifteen percent of the *CAN1* mutations in this strain background were deletions flanked by imperfect direct repeats; however, these deletions are much smaller (8 to 27 bp) than those observed in *pol3-ts1* and *-ts11*. Thus, it appears that this mutation near the C terminus of the protein primarily increases the rate of base substitutions.

We also examined the effects of these polymerase mutations on the instability of a 33-bp poly(GT) tract. This instability is measured by a frameshift assay (15) utilizing a plasmid (pSH44) containing a repetitive GT sequence fused upstream and in frame to URA3. In yeast strains transformed with this plasmid, additions or deletions of repeat units within the poly(GT) tract that result in an out-of-frame *URA3* sequence can be detected by growth in medium containing 5-FOA. This assay has previously been used to demonstrate that mutations in genes required for DNA mismatch repair (48, 51, 52) and DNA replication (*RAD27* and *POL30*) (19, 20, 22, 23, 56) significantly enhance the rate of microsatellite instability. We found that *pol3-ts1* elevates the frequency of tract instability about twofold and that neither *pol3-ts11* nor *pol3-ts26* had any significant effect (Table 5).

Effect of *msh3* mutation on accumulation of genomic deletions in *pol3-ts1* and *-ts11* strains. A possible source of the deletions observed in the strains bearing *pol3-ts1* and *-ts11* is DNA polymerase slippage. This mechanism has commonly been invoked to explain the instability of simple repetitive DNA (Fig. 2A) (53). A deletion flanked by imperfect repeats may also occur by this mechanism (Fig. 2B). Once replication proceeds through one homologous region, reannealing of separated strands may occur between the newly synthesized primer strand and a homologous region further downstream on the template, resulting in formation of a DNA loop. Failure to repair this loop would ultimately result in a deletion of the type that is prevalent in *pol3-ts1* and *-ts11* strains.

It has previously been shown that the DNA mismatch repair system efficiently corrects loops ranging from 1 to 14 nucleotides in length (49, 60). All of the deletions in the "deletions flanked by direct repeats" class in the *pol3-ts1* and *-ts11* strains were 16 bp or greater (Table 3). One explanation of this observation is that slippage events resulting in DNA loops of less than 16 bp are not observed because such loops are efficiently

repaired by the DNA mismatch repair system. This interpretation predicts that deletions of less than 16 bp would be observed in the polymerase mutant strains in the absence of DNA mismatch repair. To test this hypothesis, we combined *pol3-ts1* with a null mutation of *MSH3*, a MutS homolog that specifically functions in the correction of DNA loops up to 14 nucleotides in length (48, 49).

We found that while the mutation rate at the *CAN1* locus was unaffected by *msh3Δ* in a wild-type strain, there was a synergistic effect between *pol3-ts1* and *msh3Δ*. While the rate of mutation for *pol3-ts1* was 6-fold greater than that of the wild type, a 20-fold effect was observed for *pol3-ts1 msh3Δ* (Table 2). Sequencing of 39 Can[r] isolates from the double-mutant strain reveals two classes of mutations rarely seen in the *pol3-ts1* single mutant (Table 3). One class consists of deletions in microsatellite sequences within *CAN1* in which the size of the repeat unit ranges from 1 to 6 bp. Approximately one-half (19 of 39) of the Can[r] isolates in the *pol3-ts1 msh3* strain are of this class, which is significantly different from the frequency seen in the *pol3-ts1* single mutant ($P = 0.001$; Fisher exact test). One common deletion that appeared in 25% of the independent isolates is an $(AG)_4$ to $(AG)_3$ deletion at positions 254 to 261 of the *CAN1* open reading frame. We also transformed the *pol3-ts1 msh3* strain with pSH44 in order to assay the effects of these two mutations on the instability of a 33-bp poly(GT) tract (Table 5). We found that the effects of these two mutations are multiplicative. This strain exhibited a 150-fold enhancement in instability over the wild type for this dinucleotide repeat. Sequencing of the repeat tract from 10 independent 5-FOA[r] isolates showed that 70% of the mutations were frameshifts resulting from 2-bp deletions within the repeat tract. These results are similar to the effects seen for these two mutations on the rate of deletion formation within *CAN1* microsatellites.

The second class of mutations consists of deletions flanked by imperfect direct repeats in which the size of the deletion is less than 16 bp. These deletions were observed in approximately one-quarter (9 of 39) of the mutations in the *pol3-ts1 msh3* strain. This distribution is significantly different from that seen in the *pol3-ts1* strain, in which this deletion class is entirely absent (0 of 20) ($P = 0.02$). In addition to these two unique classes of mutations, larger deletions flanked by direct repeats persist in the *pol3-ts1 msh3* strain, but they are less frequent than in the *pol3-ts1* strain (5 of 39). In addition, the sizes of these deletions in the double-mutant strain appear to be generally smaller (16 to 38 bp) than the deletions in the *pol3-ts1* strain. We did a more limited analysis of an additional 60 independent Can[r] isolates in the *pol3-ts1 msh3* strain. Rather than sequencing all of these isolates, only those that exhibited apparent deletions by a PCR-restriction digest screen were chosen for sequencing. This screening allowed for detection of deletions as small as 8 bp by gel electrophoresis. Of these 60 isolates, 11 were deletions ranging from 8 to 14 bp and 9 were larger deletions (18 to 135 bp). The frequencies at which these classes of deletions were present were similar to those that were observed in the original 39 Can[r] isolates.

High rate of deletion formation in the *pol3-ts1* strain depends on Rad52p. To investigate the role of Rad52p in the generation of deletions in the *pol3-ts1* strain, we combined *rad52Δ* with the polymerase mutation. This double-mutant strain grew much more slowly than either of the two single-mutant strains. We also found that the effect of these two mutations on the overall mutation rate at *CAN1* was additive (Table 2). In addition, loss of Rad52p activity eliminated all of the deletions between direct repeats that are generated in the *pol3-ts1* strain (Table 3). A similar effect was previously observed when the *rfa1-29* allele was combined with *rad52Δ* (7).

TABLE 3. Mutational spectra at *CAN1* in strains with *POL3* missense mutations and/or mutations affecting DNA repair or recombination

Strain genotype[a]	Type and frequency of mutation			
	Base substitutions	Alterations within simple repeats	Deletions (bp) flanked by direct repeats	Other
WT Total	55% (11/20) C to T (3/20) T to A (2/20) G to T (2/20) G to A (2/20) T to C (1/20) C to G (1/20)	15% (3/20) G_3 to G_4 (1/20) A_6 to A_5 (1/20) A_5 to A_4 (1/20)	5% (1/20) 18 (1/20)	25% (5/20) 1-bp deletion (1/20) 5-bp insertion (1/20) 5-bp duplication (1/20)[b] 23-bp duplication (1/20) 32-bp duplication (1/20)
pol3-ts1 Total	20% (4/20) G to C (1/20) C to G (1/20) C to A (1/20) C to T (1/20)	5% (1/20) A_4 to A_3 (1/20)	65% (13/20) 16 (1/20) 18 (3/20) 38 (2/20) 42 (1/20) 49 (1/20) 51 (1/20) 59 (1/20) 99 (1/20) 108 (1/20) 336 (1/20)	10% (2/20) CCAGGT to TTCTCCA (1/20) GGT to TGG (1/20)
pol3-ts11 Total	21% (4/19) G to C (1/19) C to T (1/19) C to G (1/19) G to T (1/19)	5% (1/19) T_6 to T_5 (1/19)	58% (11/19) 16 (1/19) 18 (1/19) 27 (1/19) 34 (1/19) 38 (1/19) 49 (1/19) 142 (1/19) 239 (1/19) 662 (1/19) 804 (1/19) 864 (1/19)	16% (3/19) 1-bp deletion (1/19) 40-bp deletion (1/19) Telomere addition (1/19)[c]
pol3-ts26 Total	70% (14/20) C to G (3/20) G to C (3/20) G to A (3/20) T to A (2/20) A to T (2/20) C to T (1/20)	15% (3/20) T_6 to T_7 (1/20) A_4 to A_3 (1/20) $(GTT)_2$ to $(GTT)_1$ (1/20)	15% (3/20) 8 (1/20) 16 (1/20) 27 (1/20)	0% (0/20)
msh3Δ Total	32% (6/19) C to T (2/19) G to T (2/19) G to A (1/19) C to G (1/19)	25% (5/19) A_2 to A_1 (1/19) C_3 to C_2 (1/19) T_4 to T_3 (1/19) $(AT)_2$ to $(AT)_1$ (1/19) $(TTTA)_2$ to $(TTTA)_1$ (1/19)	11% (2/19) 8 (1/19) 10 (1/19)	32% (6/19) TTCC to CCC (1/19) TAT to CAG (1/19) 1-bp deletion (1/19) 6-bp duplication (1/19) 11-bp duplication (1/19) 49-bp duplication (1/19)
rad52Δ Total	80% (16/20) G to C (4/20) C to A (3/20) G to A (3/20) A to T (2/20) A to G (1/20) C to G (1/20) A to C (1/20) C to T (1/20)	5% (1/20) $(AT)_2$ to $(AT)_1$ (1/20)	0% (0/20)	15% (3/20) TC to AA (1/20) TTATT to ATATTT (1/20) Two base substitutions: G to A and T to A (1/20)
pol3-ts1 msh3Δ Total	13% (5/39) C to A (1/39) C to T (1/39) T to A (1/39) G to T (1/39) C to G (1/39)	49% (19/39) C_2 to C_1 (1/19) C_3 to C_2 (2/39) C_4 to C_3 (1/39) $(AG)_4$ to $(AG)_3$ (10/39) $(TTTA)_2$ to $(TTTA)_1$ (2/39)	36% (14/39) 8 (5/39) 12 (3/39) 13 (1/39) 16 (1/39) 26 (1/39)	2% (1/39) Two base substitutions: T to G and C to T (1/39)

TABLE 3—*Continued*

Strain genotype[a]	Type and frequency of mutation			
	Base substitutions	Alterations within simple repeats	Deletions (bp) flanked by direct repeats	Other
		(GGCTT)$_2$ to (GGCTT)$_1$ (1/39) (CATTAT)$_2$ to (CATTAT)$_1$ (2/39)	29 (1/39) 38 (2/39)	
pol3-ts1 rad52Δ Total	85% (17/20) C to G (6/20) T to A (3/20) G to A (2/20) C to A (2/20) G to C (2/20) A to T (1/20) T to C (1/20)	5% (1/20) T$_6$ to T$_5$ (1/20)	0% (0/20)	10% (2/20) GT$_5$GTAT to AT$_6$TTAT (1/20) 1-bp deletion (1/20)
pol3-ts1 msh3Δ rad52Δ (isolate 1) Total	61% (11/18) C to A (4/18) C to T (2/18) C to G (2/18) A to C (1/18) G to C (1/18) T to G (1/18)	17% (3/18) G$_2$ to G$_1$ (1/18) T$_4$ to T$_5$ (1/18) (AG)$_4$ to (AG)$_3$ (1/18)	11% (2/18) 12 (1/18) 16 (1/18)	11% (2/18) 1-bp deletion (2/18)
pol3-ts1 msh3Δ rad52Δ (isolate 2) Total	37% (7/19) C to T (2/19) T to G (2/19) G to T (2/19) C to G (1/19)	32% (6/19) A$_3$ to A$_4$ (1/19) G$_3$ to G$_2$ (1/19) T$_6$ to T$_5$ (1/19) T$_4$ to T$_6$ (1/19) T$_3$ to T$_2$ (1/19) (TTTA)$_2$ to (TTTA)$_1$ (1/19)	11% (2/19) 8 (1/19) 18 (1/19)	21% (4/19) TTTAAA to TTTA (1/19) C$_1$ to C$_0$ (1/19) T$_1$ to T$_0$ (1/19) A$_5$C to A$_6$G (1/19)

[a] Strain names are as follows: RJK160-1 (wild type [WT]), RJK158-3 (*pol3-ts1*), RJK187-1 (*pol3-ts11*), RJK223-1 (*pol3-ts26*), RJK357 (*msh3*), RJK334 (*rad52*), RJK358 (*pol3-ts1 msh3*), RJK288 (*pol3-ts1 rad52*), RJK363 (*pol3-ts1 msh3 rad52* isolate 1), and RJK381 (*pol3-ts1 msh3 rad52* isolate 2).

[b] All duplications had short direct repeats flanking the duplicated segment, similar to those observed in *rad27* strains (54).

[c] Telomere addition. This isolate contains a loss of chromosome V DNA up to nucleotide 34842 (as defined by Stanford *Saccharomyces* Genome Database) and the addition of a telomere of indeterminate length. The DNA sequence at this breakpoint is as follows (capital letters represent chromosome V DNA, and lowercase letters represent the new telomeric sequence): ACCTGCAGTGGAGGGTGTggtgtggtgtgtg.

These data indicate that Rad52p is required for the formation of deletions in the polymerase mutant strain.

When *rad52Δ* was combined with *pol3-ts1 msh3*, we found that for two independently derived isolates, the overall rate of mutation was identical to that of *pol3-ts1 msh3* (Table 2). In the triple-mutant strain, however, there is a significant reduction in the frequency at which frameshifts within microsatellites and deletions flanked by direct repeats are generated relative to a *pol3-ts1 msh3* strain ($P < 0.0001$ for comparison to RJK363 and $P = 0.0017$ for comparison to RJK381) (Table 3). In addition, the high rate of poly(GT) instability seen in the *pol3-ts1 msh3* strain decreased by a factor of 3 in the absence of Rad52p (Table 5).

Although *rad52Δ* in combination with *pol3-ts1* has its most striking effect on the rate of deletions, loss of Rad52p also substantially increased the rate at which base substitutions are generated in *pol3-ts1*. Most (85%) of the mutations in *pol3-ts1 rad52* were base substitutions, while only 20% of the mutations in *pol3-ts1* were of this class. Based on the overall rates of mutation and the fraction of mutations that are base substitutions for each strain, we found that the rates at which base substitutions are generated are 1.3×10^{-7} (wild type; relative rate of 1×), 2.8×10^{-7} (*pol3-ts1*; 2×), 2.2×10^{-6} (*rad52*; 17×), and 5.4×10^{-6} (*pol3-ts1 rad52*; 42×) per cell division. This result suggests that the effects of the mutant polymerase and the loss of Rad52p activity operate synergistically to generate a high rate of point mutations.

POL3 nonsense mutations exhibit a mutator phenotype and are viable as a consequence of *PSI*-mediated nonsense suppression. In addition to the missense mutants described above, we also identified five mutants (*pol3-ts8*, *-tsl5*, *-ts27*, *-ts28*, and *-ts29*) representing four unique nonsense mutants of *POL3*

TABLE 4. Sequences flanking large deletions observed in *pol3-ts1* strain

Deletion size (bp)	Sequence[a]	Extent of homology between direct repeats (bases)
16	CA<u>TGG*A*GACA</u>tctactggtgg*t*gacaAAGTTTTCGA	7 of 8
18	A<u>TTT*A*CGTTGGT</u>tcccgtattt*t*atttggtCTATCAAAG	8 of 11
18	C<u>TTCT*A*CATTGG</u>ctctctatt*at*tcattggACTTTTAGT	9 of 11
18	ATAT<u>CTCTGTTT</u>tcctgttcttagctgtttGGATCTTAT	6 of 6
38	TATTT<u>*A*CGTTGG</u>ttcc. . .gaaca*a*gttggCTCCTAAA	6 of 7
38	C<u>GTTGG*T*TCCC</u>gtat. . .caagttg*gc*tcctAAATTCCT	8 of 10
42	GTT<u>CC*A*TACAT</u>tgca. . .tttgg*ct*tacatGGAGACATC	6 of 7
49	GGTG<u>CTGGGGT</u>tacc. . .gtg*cc*tggggtCCAGGTAT	7 of 7
51	GATT<u>*A*ACGCTGC</u>cttc. . .tggt*ga*agctgcAAACCCCA	7 of 9
59	AA<u>T*GCCCGGCTT</u>ggct. . .gtt*tc*acggcttTTGCACCA	8 of 10
99	CCATACA<u>TTGCAG</u>tttt. . .ctggtgttgcagGCTTTTTT	6 of 6
108	AAAGG<u>TGGTGTT</u>ccat. . .tatcactggtgttGCAGGCTT	7 of 8
336	TG<u>TATTGG*T*TTTC</u>ttgg. . .taggttgggtttcCTCTTTGAT	8 of 9

[a] Deleted sequence is shown in lowercase. Imperfect direct repeats are underlined. Bases that differ within each repeat pair are shown in italics.

TABLE 5. Effect of *pol3* missense mutations on 33-bp dinucleotide repeat instability

Strain genotype[a]	Rate of 5-FOA[r] (10^{-6} per cell division)[b]	95% Confidence interval (10^{-6} per cell division)
WT	4.3 (1)	1.6–7.3
pol3-ts1	10 (2.3)	6.3–13
pol3-ts11	5.0 (1.2)	3.3–6.2
pol3-ts26	5.6 (1.3)	2.3–10
msh3	200 (47)	160–310
pol3-ts1 msh3	660 (150)	530–990
pol3-ts1 msh3 rad52	240 (55)	170–350

[a] Strains containing transformed pSH44 are as follows RJK242-1 (wild type [WT]), RJK166-4 (*pol3-ts1*), RJK202-3 (*pol3-ts11*), RJK232-5 (*pol3-ts26*), LS38-1 (*msh3*), LS40-1 (*pol3-ts1 msh3*), and RJK380-1 (*pol3-ts1 msh3 rad52*).
[b] Numbers given in parentheses are fold increase over wild type.

(*pol3-ts27* is equivalent to *pol3-ts29*). The positions of these mutations are shown in Fig. 1. One mutant (*pol3-17*), which was not investigated further, had three mutant substitutions (silent mutation at Y336, L781F, and Q963UAA). All four nonsense mutants examined were temperature sensitive and MMS sensitive (Fig. 3). In addition, a large fraction of large budded cells were observed at both 30 and 37°C. The percentages of cells with this morphology at 30°C for the wild type and *pol3-ts8, -ts15, -ts28,* and *-ts29* were 7, 37, 35, 42, and 39%, respectively (500 cells were counted). After incubation of the cells at 37°C for 20 h, the percentages of cells with this morphology for the wild type and *pol3-ts8, -ts15, -ts28,* and *-ts29* were 6, 83, 42, 83, and 65%, respectively (500 cells were counted). The *pol3-ts15* mutant had a smaller fraction of large-budded cells than the other mutants at 37°C and also displayed a less severe growth defect at this temperature than the other mutants.

Each of these nonsense mutants elevated the rate of mutation at the *CAN1* locus between 5- and 14-fold. The mutation rates (all 10^{-7}/cell division; 95% confidence limits are shown in parentheses) for the wild type and *pol3-ts8, -ts15, -ts28,* and *-ts29* were 2.4 (2.3 to 2.9), 20 (17 to 22), 12 (8 to 14), 20 (16 to 26), and 33 (30 to 55). We examined the mutational spectra at *CAN1* for the nonsense mutants *pol3-ts8* and *pol3-ts15*. As was

observed for *pol3-ts1* and *pol3-ts11*, over one-half of the mutations within *CAN1* generated in strains bearing either of these two nonsense mutations were deletions of 16 bp or greater (Table 6) flanked by imperfect direct repeats (data not shown). One mutation identified in the *pol3-ts8* strain had a deletion followed by a telomere addition that was similar to one of the observed mutations in the *pol3-ts11* strain.

Since *POL3* is an essential gene and several of the mutations were located upstream of the catalytic domain of Pol3p, our recovery of viable cells with these mutations was very surprising. One plausible explanation for viability, the existence of a nonsense-suppressing tRNA gene in the genetic background, was unlikely, since such suppressors in yeasts are codon specific (17) and we had identified both amber (UAG) and ochre (UAA) *pol3* mutants.

A different type of suppressor, which can elevate the readthrough of all nonsense codons, is the prion-like [*PSI*⁺] factor (31, 32, 59). The [*PSI*⁺] factor, encoded by the *SUP35* gene, is a misfolded form of the translational termination factor eRF-3. [*PSI*⁺] can be cured from a yeast strain by plating cells on enriched medium containing low levels of GuHCl (59). To test for the presence of a [*PSI*⁺]-like element in our host strain, we examined the viability of the strains containing the *POL3* nonsense mutations on medium containing GuHCl. We found that all of the temperature-sensitive *POL3* nonsense mutants failed to grow on enriched medium containing GuHCl while an isogenic *POL3*⁺ strain and all of the *POL3* missense mutants grew normally (data not shown). Since loss of viability under growth conditions that cure yeast of [*PSI*⁺] was specific to the presence of *POL3* nonsense mutations, it appears that [*PSI*⁺]-mediated nonsense suppression is responsible for the viability of strains containing these *POL3* mutations.

Reduced expression of *POL3* elevates mutation rates. There are two explanations of the mutator phenotype exhibited by the *pol3* nonsense mutations. Since [*PSI*⁺]-mediated suppression involves the insertion of an amino acid in place of the termination codon, this substitution may yield a mutator DNA polymerase. Alternatively, since the efficiency of [*PSI*⁺]-mediated suppression in yeast is reported to be very low (~1%) (30), the mutator phenotype may reflect a very low level of fully functional DNA polymerase. To distinguish between

TABLE 6. Mutational spectra at *CAN1* in strains with *POL3* nonsense mutations

Strain genotype[a]	Type and frequency of mutation			
	Base substitutions	Alterations within simple repeats	Deletions (bp) flanked by direct repeats	Other
pol3-ts8 Total	22% (2/9) C to A (1/9) A to T (1/9)	11% (1/9) (AT)$_2$ to (AT)$_1$ (1/9)	56% (5/9) 18 (1/9) 27 (1/9) 30 (1/9) 38 (1/9) 662 (1/9)	11% (1/9) Telomere addition (1/9)[b]
pol3-ts15 Total	33% (3/9) C to T (1/9) G to A (1/9) C to G (1/9)	0% (0/9)	56% (5/9) 16 (2/9) 18 (1/9) 268 (1/9) 426 (1/9)	11% (1/9) 17-bp duplication (1/9)[c]

[a] Strain names are as follows: RJK185-1 (*pol3-ts8*) and RJK218-2 (*pol3-ts15*).
[b] Telomere addition. This isolate contains a loss of chromosome V DNA up to nucleotide 34831 (as defined by Stanford *Saccharomyces* Genome Database) and the addition of a telomere of indeterminate length. The DNA sequence at this breakpoint is as follows (capital letters represent chromosome V DNA, and lowercase letters represent the new telomeric sequence): GTGGAGGGTGTTGTTGTGGAGTgggtgtggtgtgtg.
[c] All duplications had short direct repeats flanking the duplicated segment, similar to those observed in *rad27* strains (54).
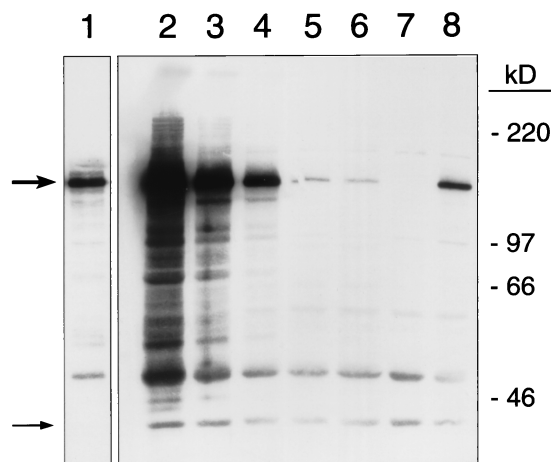
FIG. 4. Effect of galactose concentration on Pol3p levels in *GAL1-POL3* strain. Cell lysates were prepared and probed for 3×HA-Pol3p by Western blot analysis as described in Materials and Methods. The location of 3×HA-Pol3p is indicated with a thick arrow, and the position of a protein nonspecifically recognized by the HA antibody (used as a loading control) is indicated with a thin arrow. The positions of the molecular mass standards are shown on the right. Lanes 1 to 6 contain lysates of RJK368-4 (*GAL1-3×HA-POL3 pep4*) grown in enriched medium containing 3% raffinose and the following galactose concentrations: lanes 1 and 2, 0.5%; lane 3, 0.05%; lane 4, 0.01%; lane 5, 0.005%; lane 6, no galactose. Lane 7 contains a lysate of RJK366-5 (*POL3 pep4*) grown in 2% glucose; lane 8 contains a lysate of RJK394 (*3×HA-POL3 pep4*) grown in 2% glucose. The lysates in lanes 7 and 8 are from strains in which *POL3* transcription is driven from the native *POL3* promoter. The amount of lysate loaded was approximately 30 μg in lanes 2 to 8 and 6 μg in lane 1. The band pattern shown in lane 1 was generated from a much shorter film exposure than those shown in lanes 2 to 8. The intensities of the Pol3p bands in lanes 2 to 6 relative to the Pol3p band intensity in lane 8 are 32, 11, 2.8, 0.084, and 0.060, respectively. Similar relative intensities derived from a second independent set of lysates were 6.1, 3.0, 3.0, 0.052, and 0.022. From a third set of lysates, the relative intensities of the Pol3p band for the samples in lanes 2 and 3 were 44 and 11, respectively. Averages among all the data sets for each growth condition are presented in Results.

these alternatives, we replaced the native promoter of *POL3* with the galactose-inducible *GAL1/10* promoter; in addition, we inserted an epitope tag (HA) at the beginning of the gene in order to monitor the level of the protein. From previous studies, it has been shown that the level of gene expression from the *GAL1/10* promoter can be regulated by altering the concentration of galactose (3). In most of our experiments, cells were grown in a constant level of the noninducing carbon source raffinose (3%) and the level of galactose was varied from 0.5 to 0%. In a few experiments, we grew cells in 2% glucose. In glucose-containing medium, the level of expression from the *GAL1/10* promoter is even lower than that from cells grown in 3% raffinose in the absence of glucose because glucose-grown cells repress expression of the *GAL1/10* promoter (45).

To monitor the level of DNA polymerase δ, we performed Western blot analysis (using antibodies directed against the HA epitope) on protein extracts of cells grown in various types of media. As expected, the level of DNA polymerase δ was related to the concentration of galactose in the medium (Fig. 4). As a control, we monitored the level of DNA polymerase δ in a strain in which the same HA tag was inserted into a *POL3* gene with its native promoter (Fig. 4, lane 8). Giving the level of DNA polymerase in this control strain a value/1, the approximate levels of DNA polymerase in cells grown in 3% raffinose plus 0.5% galactose (lanes 1 and 2), 3% raffinose plus 0.05% galactose (lane 3), 3% raffinose plus 0.1% galactose (lane 4), 3% raffinose plus 0.005% galactose (lane 5), and 3% raffinose without galactose (lane 6) were 27, 8, 3, 0.07, and 0.04, respectively.

The effects of reducing *POL3* expression on cell growth and sensitivity to DNA damage were evaluated. When it was grown with reduced levels of galactose (0.005%), we found the yeast strain containing this *GAL1-POL3* construct exhibited a fairly high level of sensitivity to MMS but no apparent UV sensitivity (Fig. 5). In addition, cell viability was sensitive to the level of DNA polymerase δ in the absence of Rad52p. As shown in Fig. 6, lowering the galactose concentration from 0.05 to 0.005% noticeably lowered the ability of a *GAL1-POL3 rad52Δ* strain to sustain growth. One interpretation of this result is that a reduction in the level of DNA polymerase δ leads to an increase in the level of DNA double-strand breaks.

Surprisingly, we observed no apparent loss in viability or temperature sensitivity when the growth medium contained low levels of galactose in a *RAD52* strain with the *GAL1-POL3* construct (RJK398) (Fig. 6 and data not shown). There was, however, a larger percentage of large-budded cells (40%) present during growth with 0.005% galactose compared to that seen during growth with 0.05% galactose (10% large-budded cells). In the absence of galactose (3% raffinose), a condition in which there is a very low level of DNA polymerase δ, the growth rate is substantially reduced at both 30 and 37°C, although there was still no apparent temperature sensitivity under these growth conditions. In addition, a much higher percentage of cells grown in the absence of galactose are large budded (65%). Furthermore, most of the unbudded cells are enlarged and irregular in shape. The above-mentioned growth defects in the absence of galactose are further exacerbated when this strain is grown in enriched medium containing only glucose (YPD). Cells incubated in YPD medium grew very slowly and were not further evaluated.

When the strain bearing the *GAL1-POL3* construct was examined for the *CAN1* mutation rate, we observed a gradual increase in the mutator phenotype as the level of Pol3p was reduced. The rates of *can1* mutations in the strain with the *GAL1/10-POL3* gene (all 10^{-7}/cell division; 95% confidence limits are in parentheses) when grown in 3% raffinose plus 0.5% galactose, 3% raffinose plus 0.05% galactose, 3% raffinose plus 0.01% galactose, 3% raffinose plus 0.005% galactose, and 3% raffinose without galactose were 1.5 (1.3 to 1.6), 1.7 (1.6 to 2.1), 5.6 (4.9 to 7.4), 15 (11 to 18), and 56 (43 to 95), respectively. When the strain with the HA-tagged *POL3* gene and the native promoter was grown in 3% raffinose plus 0.05% galactose, 3% raffinose without galactose, and YPD medium, the mutation rates (all 10^{-7}/cell division; 95% confidence limits are in parentheses) were 2.6 (2.2 to 3.6), 2.6 (2.1 to 3.6), and 4.4 (3.4 to 5.7), respectively. Finally, when a strain with an untagged version of the *POL3* gene with its native promoter was grown in medium containing 3% raffinose plus 0.05% galactose, we observed a rate of mutation of 1.4 (1.1 to 1.9) $\times 10^{-7}$/cell division. We conclude from these studies that reducing the level of fully functional DNA polymerase δ can substantially elevate global mutation rates, whereas overexpression of DNA polymerase δ does not result in a mutator phenotype.

We also examined the spectra of mutations generated in cells with low levels of DNA polymerase (Table 7). Although cells grown in medium with 3% raffinose plus 0.05% galactose (no mutator effect) had a spectrum of alterations similar to that observed in the wild-type strain, the same strain grown in medium with 3% raffinose and 0.005% galactose or no galactose had a significantly elevated frequency of deletions between direct repeats. Thus, the mutator phenotype in strains with reduced levels of Pol3p resembles that observed for some of the *POL3* missense mutations and the *POL3* nonsense mutations.
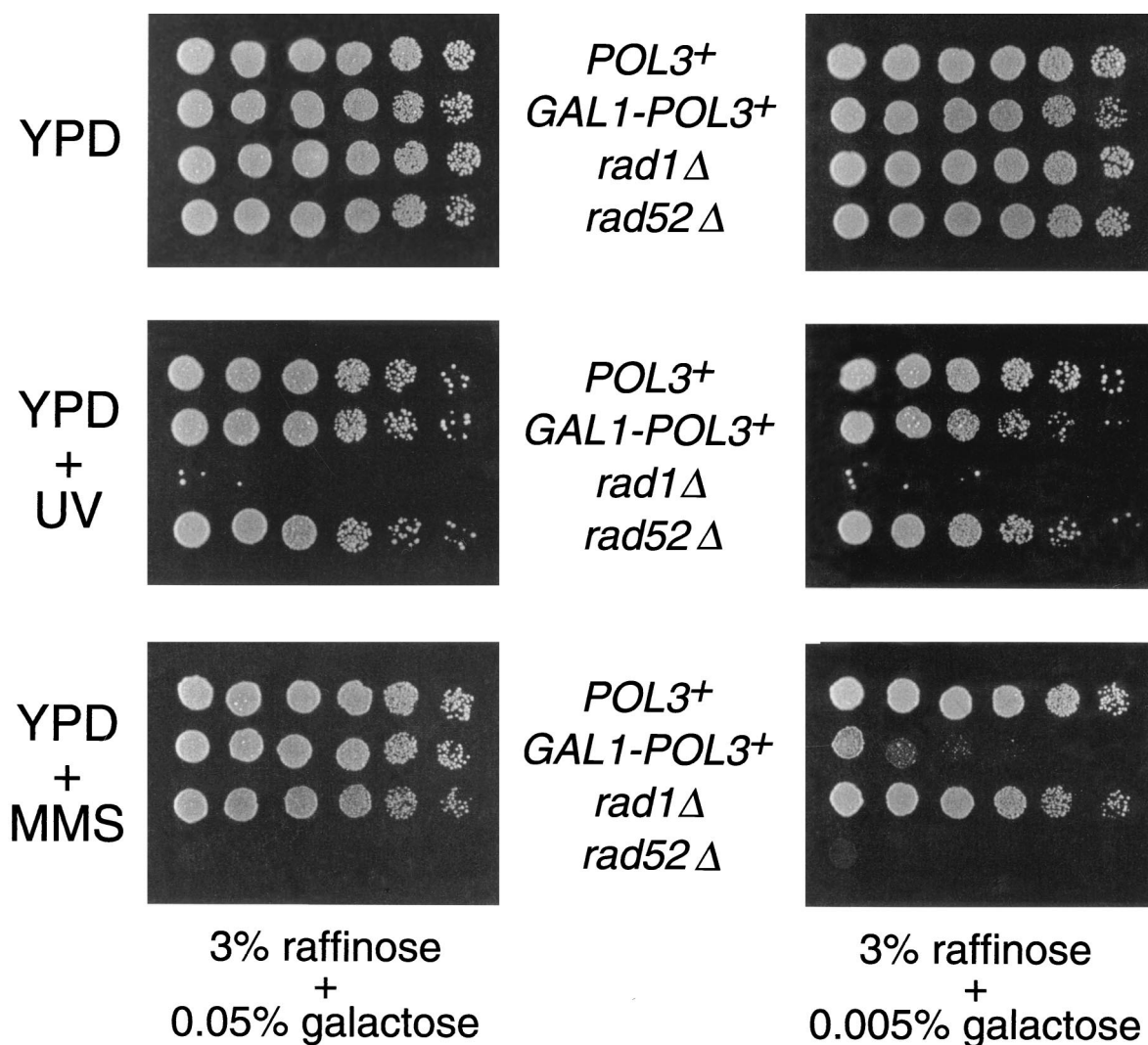
FIG. 5. Effects of a reduction in the level of DNA polymerase δ on DNA repair processes. Fivefold serial dilutions of strains MS71 (*POL3*; top row of each panel), RJK341 (*GAL1-POL3*; second row), EAS102 (*rad1Δ*; third row), and HM6 (*rad52Δ*; bottom row) were spotted onto YPR plates containing the indicated concentrations of galactose in the presence of MMS or subjected to UV irradiation.

DISCUSSION

The low level of mutations observed in wild-type cells is a consequence of the serial operation of multiple levels of control of the accuracy of DNA replication: base selectivity by DNA polymerase, exonucleolytic proofreading, and postreplicative DNA mismatch repair (44). If frameshifts within simple repetitive DNA sequences and deletions between direct repeats reflect DNA polymerase slippage events, the low level of such alterations in wild-type cells is likely to reflect the processivity of replicative DNA polymerases and the efficiency of postreplicative DNA mismatch repair. One might expect, therefore, mutator alleles of DNA polymerase that reduce base selectivity, the efficiency of proofreading, or the processivity of replication. In addition, a DNA polymerase mutation could indirectly result in a mutator phenotype. For example, if the level of an accurate replicative DNA polymerase was lowered, its role could be partially taken over by an error-prone DNA polymerase.

One of the *POL3* missense mutants, *pol3-ts26*, elevated the rate of base substitution mutations with only a minor effect on the rate of deletions. This mutant polymerase could have a partial defect in base selectivity or proofreading. Strains with the other two missense mutations (*pol3-ts1* and *pol3-ts11*), the nonsense *pol3* mutations, or reduced levels of DNA polymerase δ had elevated levels of deletions, as well as base pair substitutions; these deletions, like those observed in *rfa1* strains (7), involved interactions between short dispersed repeats.

Mechanism of deletion formation. Deletions could result from DNA polymerase slippage (Fig. 2B) or single-strand annealing (SSA) (Fig. 2C). Our conclusion that many of the deletions result from DNA polymerase slippage is based primarily on a comparison of the sizes of the deletions generated in *pol3* mutant strains and in strains with both *pol3* and *msh3* mutations. In single-mutant *pol3-ts1* and *pol3-ts11* strains, all deletion mutations involving the *CAN1* locus were single-base-pair deletions in homopolymeric regions or deletions of at least 16 bp. In contrast, in a strain with both the *pol3-ts1* and *msh3* mutations, over 70% of the deletions were more than 1 bp but less than 16 bp (Table 3). Msh3p is involved in the repair of DNA loops ranging in size from 1 to 14 bp (48, 60). We sug-

3% raffinose
+
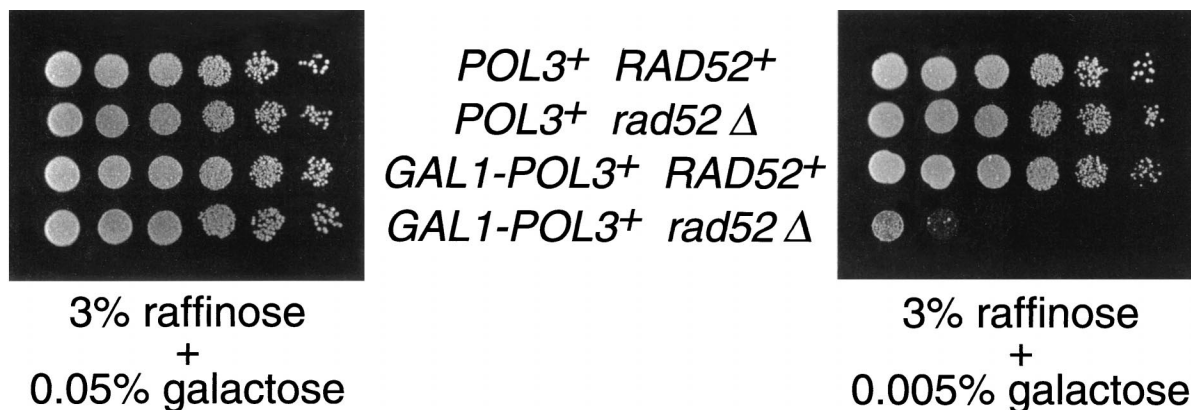0.05% galactose

3% raffinose
+
0.005% galactose

FIG. 6. A reduction in the level of Pol3p reduces cell viability in the absence of Rad52p. Fivefold serial dilutions of strains RJK396 (*POL3 RAD52*; top row of each panel), RJK397 (*POL3 rad52Δ*; second row), RJK398 (*GAL1-POL3 RAD52*; third row), and RJK399 (*GAL1-POL3 rad52Δ*; bottom row) were spotted onto plates containing the indicated medium. All four strains were derived from the same tetrad following sporulation and dissection of diploid strain RJK372. The growth pattern shown here is identical to that from two additional tetrads of the same genotypes.

gest, therefore, that the *pol3-ts1* and *pol3-ts11* mutations result in increased levels of DNA polymerase slippage and increased rates of formation of DNA loops. Since DNA loops smaller than 16 bp are efficiently corrected in single-mutant *pol3* strains, we observe an increase in mutation frequency only in deletions of 16 bp or larger. In the double-mutant *pol3 msh3* strains, deletions of both classes are observed, as expected by the DNA polymerase slippage model. This model also predicts the synergistic effect of *pol3-ts1* and *msh3* on mutation rates at the *CAN1* locus and the synergistic destabilization of the poly(GT) tract.

An alternative model for the generation of deletions is by SSA (Fig. 2C). Although SSA requires *MSH3* (as well as *MSH2*, *RAD1*, and *RAD10*), if the distance between interacting repeats is greater than 60 bp (39), deletions smaller than 60 bp could be generated by this mechanism. However, since this mechanism does not explain the lack of deletions of less than 16 bp in the *pol3-ts1* strain and the prevalence of these deletions in the *pol3-ts1 msh3* strain, we prefer the DNA polymerase slippage model. Several additional points concerning this conclusion should be mentioned. First, our conclusion is rig-

TABLE 7. Effect of *POL3* expression level on mutational spectra at *CAN1* in yeast strain RJK341

Growth media	Type and frequency of mutation			
	Base substitutions	Alterations within simple repeats	Deletions (bp) flanked by direct repeats	Other
YPR + 0.05% galactose Total	84% (16/19) G to T (4/19) G to A (3/19) C to T (3/19) C to A (2/19) A to T (1/19) T to C (1/19) T to G (1/19) T to A (1/19)	0% (0/19)	5% (1/19) 206 (1/19)	11% (2/19) ATA to TT (1/19) TT to ATA (1/19)
YPR + 0.005% galactose Total	32% (6/19) G to C (2/19) T to A (2/19) C to G (1/19) C to T (1/19)	5% (1/19) T_5 to T_4 (1/19)	58% (11/19) 15 (1/19) 16 (2/19) 18 (2/19) 24 (1/19) 39 (1/19) 49 (1/19) 53 (2/19)	5% (1/19) 1-bp deletion (1/19)
YPR Total	40% (8/20) G to C (3/20) T to A (2/20) C to G (1/20) A to T (1/20) C to A (1/20)	5% (1/20) A_5 to A_6 (1/20)	45% (9/20) 8 (2/20) 16 (2/20) 17 (1/20) 29 (1/20) 59 (1/20) 81 (1/20) 1,077 (1/20)	10% (2/20) GTA to TTT (1/20) Two base substitutions: A to C and G to C (1/20)

orous only for deletions of 16 bp or less, although it seems reasonable that somewhat larger deletions are also generated by DNA polymerase slippage. Second, it is likely that very large deletions (greater than 1 kb) represent SSA events. Chen et al. (7) found that a mutant allele of *RFA1* elevated frequencies of large deletions (mostly larger than 6 kb) in the *CAN1* locus; they reported that deletion formation was dependent on Rad10p, as expected for SSA events. It should be pointed out that, although Rad1p and Rad10p have roles in the meiotic repair of large DNA loops (21), *rad1* strains do not appear to be deficient in the mitotic repair of large DNA loops (E. Sia and T. Petes, unpublished data).

Rad52p is required for most types of homologous recombination in yeast, including SSA (40). In strains with mutations in *POL3* and *RAD52*, very few deletions are observed. This observation can be interpreted in two ways. One possibility is that deletions are generated by SSA; as described above, this possibility is unlikely for deletions of less than 16 bp. An alternative possibility is that Rad52p promotes DNA polymerase slippage between short dispersed repeats. Following DNA strand dissociation, Rad52p could help the nascent strand seek out regions of homology in single-stranded regions of the replication fork. Using a different assay for mutations, Tran et al. (55) observed Rad52p dependence of deletion formation and suggested a nonrecombinational role for Rad52p in this process.

We observed a substantial increase in the rate of base substitutions in a *rad52Δ* strain and a synergistic effect between *pol3-ts1* and *rad52*. It has previously been shown that loss of Rad52p function also increases the rate of base substitutions at the *SUP4* locus and that this increase is dependent on the presence of the error-prone DNA polymerase ζ (42). Since DNA polymerase ζ normally functions in translesion DNA synthesis (11), the elevated mutation rates observed in the *rad52Δ* strain may be a consequence of error-prone repair synthesis at regions of spontaneous DNA damage. The synergistic effect of *pol3-ts1* and *rad52Δ* on the rate of base substitutions may reflect an increase in DNA damage associated with the *pol3-ts1* mutation.

One interpretation of the phenotypes associated with the *pol3-ts1* and *-ts11* mutations is that the mutant polymerases are less processive. Reduced processivity associated with phage T7 DNA polymerase lacking the processivity factor thioredoxin and a mutant of the Klenow fragment DNA polymerase has been correlated with increased microsatellite instability (26, 36). For the yeast DNA polymerase mutants, reductions in processivity may be a consequence of defective interactions with the processivity factor PCNA. Regions within the N-terminal region of Pol3p appear to interact with PCNA, and the processivity of DNA polymerase δ depends on this interaction (5, 61). Alternatively, increases in frameshift mutagenesis could reflect defective interactions within the polymerase active site, as observed for a mutant human DNA polymerase β (38). A final alternative is that the *pol3-ts1* and *-ts11* mutations result in lower levels of DNA polymerase, producing a mutator phenotype by the mechanisms described below for strains with low levels of DNA polymerase δ.

Nonsense mutations of *POL3*. We recovered viable *POL3* nonsense mutations because of [*PSI*]-mediated readthrough of the nonsense codons. Since this suppression is inefficient (30), the mutator phenotype of the *POL3* nonsense mutations (increased frequencies of deletions with a smaller effect on base pair substitutions) presumably reflects the same mechanisms (described below) observed in strains with low levels of DNA polymerase δ. The temperature-sensitive phenotype of the nonsense mutations is likely to be a consequence of the temperature-sensitive efficiency of [*PSI*]-dependent nonsense suppres-

sion (18). One interesting consequence of this mechanism is the fact that, in strains with the nonsense *POL3* mutations, the [*PSI*] factor (usually dispensable) is essential.

Mutator phenotype generated by depleted levels of DNA polymerase δ. When the level of DNA polymerase δ was reduced, we observed elevated rates of deletions (presumably reflecting elevated rates of DNA polymerase slippage) and base pair substitutions. Since slippage could occur during the transition between discontinuous synthesis (associated with dissociation of DNA polymerase α from the template) and continuous synthesis (associated with attachment of DNA polymerase δ to the template), a reduction in the level of wild-type DNA polymerase molecules could result in increased slippage. Similarly, delayed DNA synthesis on the lagging strand could lead to increased single-stranded regions in the replication fork and the opportunity for the occurrence of slippage events that involve dispersed small repeats, resulting in deletions.

Although there is a strong inverse correlation between polymerase levels and mutation rates in the *GAL1-POL3* strain, there is one apparent discrepancy. Growth of this strain in YPR medium containing 0.01% galactose results in a threefold increase in the level of DNA polymerase δ over that observed in a strain in which *POL3* is normally expressed under the control of its native promoter. However, the mutation rate of the *GAL1-POL3* strain under these growth conditions is twice that of the normal observed rate. One possible explanation is that *GAL1-POL3* expression is constitutive while *POL3* expression under its native promoter occurs primarily during S phase.

Although the most obvious mutator phenotype of reducing the level of DNA polymerase δ was an effect on the rate of deletion formation, base pair substitutions were also elevated. If reducing the level of DNA polymerase δ increases the size of single-stranded regions at the replication fork, there may be more spontaneous DNA damage. Such damage could have two consequences: (i) reduction in viability in strains with a *rad52* mutation (as observed) and (ii) increased levels of mutations resulting from repair of damaged DNA by an error-prone DNA polymerase, such as DNA polymerase ζ. It is somewhat surprising that gross overproduction of DNA polymerase δ had no mutator phenotype, since dominant-negative effects caused by overproducing one subunit of a multienzyme complex are quite common in yeast (41).

Our observations may be relevant to understanding certain human diseases associated with genomic instability. One type of genomic instability (microsatellite instability) in patients with hereditary nonpolyposis colorectal cancer is associated with mutations in genes involved in DNA mismatch repair (9). We suggest that mutator variants of DNA polymerase δ or epigenetic reduction in the level of DNA polymerase δ could be another source of genome destabilization. Mutations of the human DNA polymerase δ gene have been detected in cancer cell lines, although the functional significance of these mutations has not yet been established (10). In order for mutations in DNA polymerase genes to promote tumor formation, they would need to have a strong mutator phenotype without a strong growth defect, possibly a difficult balance to achieve.

REFERENCES

1. **Alani, E. A., L. Cao, and N. Kleckner.** 1987. A method for gene disruption that allows repeated use of *URA3* selection in the construction of multiply disrupted yeast strains. Genetics **116:**541–545.
2. **Alarcon, C. M., J. Heitman, and M. E. Cardenas.** 1999. Protein kinase activity and identification of a toxic effector domain of the target of rapamycin TOR proteins in yeast. Mol. Biol. Cell. **10:**2531–2546.
3. **Aparicio, O. M., and D. E. Gottschling.** 1994. Overcoming telomeric silencing: a trans-activator competes to establish gene expression in a cell cycle-dependent way. Genes Dev. **8:**1133–1146.
4. **Boeke, J. D., F. Lacroute, and G. R. Fink.** 1984. A positive selection for mutants lacking orotidine-5′-phosphate decarboxylase activity in yeast: 5-fluoroorotic acid resistance. Mol. Gen. Genet. **167:**345–346.
5. **Brown, W. C., and J. L. Campbell.** 1993. Interaction of proliferating cell nuclear antigen with yeast DNA polymerase δ. J. Biol. Chem. **268:**21706–21710.
6. **Chen, C., and R. D. Kolodner.** 1999. Gross chromosomal rearrangements in *Saccharomyces cerevisiae* replication and recombination defective mutants. Nat. Genet. **23:**81–85.
7. **Chen, C., K. Umezu, and R. D. Kolodner.** 1998. Chromosomal rearrangements occur in *S. cerevisiae rfa1* mutator mutants due to mutagenic lesions processed by double-strand-break repair. Mol. Cell **2:**9–22.
8. **Chen, C., B. J. Merrill, P. L. Lau, C. Holm, and R. D. Kolodner.** 1999. *Saccharomyces cerevisiae pol30* (proliferating cell nuclear antigen) mutations impair replication fidelity and mismatch repair. Mol. Cell. Biol. **19:**7801–7815.
9. **Eshleman, J. R., and S. D. Markowitz.** 1995. Microsatellite instability in inherited and sporadic neoplasms. Curr. Opin. Oncol. **7:**83–89.
10. **Flohr, T., J. C. Dai, J. Buttner, O. Popanda, E. Hagmuller, and H. W. Thielmann.** 1999. Detection of mutations in the DNA polymerase δ gene of human sporadic colorectal cancers and colon cancer cell lines. Int. J. Cancer **80:**919–929.
11. **Friedberg, E. C., and V. L. Gerlach.** 1999. Novel DNA polymerases offer clues to the molecular basis of mutagenesis. Cell **98:**413–416.
12. **Gordenin, D. A., A. L. Malkova, A. Peterzen, V. N. Kulikov, Y. I. Pavlov, E. Perkins, and M. A. Resnick.** 1992. Transposon Tn*5* excision in yeast: influence of DNA polymerases α, δ, and ε repair genes. Proc. Natl. Acad. Sci. USA **89:**3785–3789.
13. **Habraken, Y., P. Sung, L. Prakash, and S. Prakash.** 1996. Binding of insertion/deletion DNA mismatches by the heterodimer of yeast mismatch repair proteins MSH2 and MSH3. Curr. Biol. **6:**1185–1187.
14. **Hartwell, L. H.** 1976. Sequential function of gene products relative to DNA synthesis in the yeast cell cycle. J. Mol. Biol. **104:**803–817.
15. **Henderson, S., and T. D. Petes.** 1992. Instability of simple sequence DNA in *Saccharomyces cerevisiae*. Mol. Cell. Biol. **12:**2749–2757.
16. **Hindges, R., and U. Hubscher.** 1997. DNA polymerase δ, an essential enzyme for DNA transactions. Biol. Chem. **378:**345–362.
17. **Hinnebusch, A. G., and S. W. Liebman.** 1991. Protein synthesis and translational control in *Saccharomyces cerevisiae*, p. 627–735. *In* J. R. Broach, J. R. Pringle, and E. W. Jones, (ed.), The molecular and cellular biology of the yeast Saccharomyces: genome dynamics, protein synthesis, and energetics. Cold Spring Harbor Laboratory, Cold Spring Harbor, N.Y.
18. **Inge-Vechtomov, S. G., L. N. Mironova, and M. D. Ter-Avanesian.** 1994. Ambiguity of translation: an eukaryotic version? Russian J. Genet. **30:**890–902.
19. **Johnson, R. E., G. K. Kovvali, L. Prakash, and S. Prakash.** 1995. Requirement of the yeast *RTH1* 5′ to 3′ exonuclease for the stability of simple repetitive DNA. Science **269:**238–240.
20. **Johnson, R. E., G. K. Kovvali, S. N. Guzder, N. S. Amin, C. Holm, Y. Habraken, P. Sung, L. Prakash, and S. Prakash.** 1996. Evidence for involvement of yeast proliferating cell nuclear antigen in DNA mismatch repair. J. Biol. Chem. **271:**27987–27990.
21. **Kirkpatrick, D., and T. D. Petes.** 1997. Repair of DNA loops involves DNA mismatch and nucleotide excision repair proteins. Nature **387:**929–931.
22. **Kokoska, R. J., L. Stefanovic, H. T. Tran, M. A. Resnick, D. A. Gordenin, and T. D. Petes.** 1998. Destabilization of yeast micro- and minisatellite DNA sequences by mutations affecting a nuclease involved in Okazaki fragment processing (*rad27*) and DNA polymerase δ (*pol3-t*). Mol. Cell. Biol. **18:**2779–2788.
23. **Kokoska, R. J., L. Stefanovic, A. B. Buermeyer, R. M. Liskay, and T. D. Petes.** 1999. A mutation of the yeast gene encoding PCNA destabilizes both microsatellite and minisatellite DNA sequences. Genetics **151:**511–519.
24. **Kolodner, R.** 1996. Biochemistry and genetics of eukaryotic mismatch repair. Genes Dev. **10:**1433–1442.
25. **Kramer, K. M., and J. E. Haber.** 1993. New telomeres in yeast are initiated with a highly selected subset of $TG_{1–3}$. Genes Dev. **7:**2345–2356.
26. **Kunkel, T. A., S. S. Patel, and K. A. Johnson.** 1994. Error-prone replication of repeated DNA sequences by T7 DNA polymerase in the absence of its processivity unit. Proc. Natl. Acad. Sci. USA **91:**6830–6834.
27. **Kunz, B. A., K. Ramachandran, and E. J. Vonarx.** 1998. DNA sequence analysis of spontaneous mutagenesis in *Saccharomyces cerevisiae*. Genetics **148:**1491–1505.

28. **Lea, D. E., and C. A. Coulson.** 1949. The distribution of the number of mutants in bacterial populations. J. Genet. **49:**264–285.
29. **Lew, D. J., T. Weinert, and J. R. Pringle.** 1997. Cell cycle control in *Saccharomyces cerevisiae*, p. 607–695. *In* J. R. Pringle, J. R. Broach, and E. W. Jones (ed.), The molecular and cellular biology of the yeast Saccharomyces: cell cycle and cell biology. Cold Spring Harbor Laboratory, Cold Spring Harbor, N.Y.
30. **Liebman, S. W., and F. Sherman.** 1979. Extrachromosomal *PSI*⁺ determinant suppresses nonsense mutations in yeast. J. Bacteriol. **139:**1068–1071.
31. **Lindquist, S.** 1997. Mad cows meet psi-chotic yeast: the expansion of the prion hypothesis. Cell **89:**495–498.
32. **Lindquist, S., M. M. Patino, Y. O. Chernoff, A. S. Kowal, M. A. Singer, S. W. Liebman, K. H. Lee, and T. Blake.** 1995. The role of Hsp104 in stress tolerance and [PSI⁺] propagation in *Saccharomyces cerevisiae*. Cold Spring Harbor Symp. Quant. Biol. **60:**451–460.
33. **Liu, V. F., D. Bhaumik, and T. S.-F. Wang.** 1999. Mutator phenotype induced by aberrant replication. Mol. Cell. Biol. **19:**1126–1135.
34. **Longtine, M. S., A. McKenzie III, D. J. Demarini, N. G. Shah, A. Wach, A. Brachat, P. Philippsen, and J. R. Pringle.** 1998. Additional modules for versatile and economical PCR-based gene deletion and modification in *Saccharomyces cerevisiae*. Yeast **14:**953–961.
35. **Marsischky, G. T., N. Filosi, M. F. Kane, and R. D. Kolodner.** 1996. Redundancy of *Saccharomyces cerevisiae* MSH3 and MSH6 in MSH2-dependent mismatch repair. Genes Dev. **10:**407–420.
36. **Minnick, D. T., M. Astatke, C. M. Joyce, and T. A. Kunkel.** 1996. A thumb subdomain mutant of the large fragment of *Escherichia coli* DNA polymerase I with reduced DNA binding affinity, processivity, and frameshift fidelity. J. Biol. Chem. **271:**24954–24961.
37. **Morrison, A., and A. Sugino.** 1994. The 3′ to 5′ exonucleases of both DNA polymerases δ and ε participate in correcting errors in DNA replication in *Saccharomyces cerevisiae*. Mol. Gen. Genet. **242:**289–296.
38. **Osheroff, W. P., W. A. Beard, S. Yin, S. H. Wilson, and T. A. Kunkel.** Minor groove interactions at the DNA polymerase β active site modulate single-base deletion error rates. J. Biol. Chem., in press.
39. **Paques, F., and J. E. Haber.** 1997. Two pathways for removal of nonhomologous DNA ends during double-strand break repair in *Saccharomyces cerevisiae*. Mol. Cell. Biol. **17:**6765–6771.
40. **Paques, F., and J. E. Haber.** 1999. Multiple pathways of recombination induced by double-strand breaks in *Saccharomyces cerevisiae*. Microbiol. Mol. Biol. Rev. **63:**349–404.
41. **Rine, J.** 1991. Gene overexpression in studies of *Saccharomyces cerevisiae*, p. 239–251. *In* C. Guthrie and G. R. Fink (ed.), Guide to yeast genetics and molecular biology. Academic Press, San Diego, Calif.
42. **Roche, H., R. D. Gietz, and B. A. Kunz.** 1995. Specificities of the *Saccharomyces cerevisiae rad6, rad18,* and *rad52* mutators exhibit different degrees of dependence on the *REV3* gene product, a putative nonessential DNA polymerase. Genetics **140:**443–456.
43. **Sambrook, J., E. F. Fritsch, and T. Maniatis.** 1989. Molecular cloning: a laboratory manual, 2nd ed. Cold Spring Harbor Laboratory, Cold Spring Harbor, N.Y.
44. **Schaaper, R. M.** 1993. Base selection, proofreading, and mismatch repair during DNA replication in *Escherichia coli*. J. Biol. Chem. **268:**23762–23765.
45. **Schneider, J. C., and L. Guarente.** 1991. Vectors for expression of cloned genes in yeast: regulation, overproduction, and underproduction, p. 373–388. *In* C. Guthrie and G. R. Fink (ed.), Guide to yeast genetics and molecular biology. Academic Press, San Diego, Calif.
46. **Sherman, F.** 1991. Getting started with yeast, p. 3–21. *In* C. Guthrie and G. R. Fink (ed.), Guide to yeast genetics and molecular biology. Academic Press, San Diego, Calif.
47. **Sia, E. A., S. Jinks-Robertson, and T. D. Petes.** 1997. Genetic control of microsatellite stability. Mutat. Res. **383:**61–70.
48. **Sia, E. A., R. J. Kokoska, M. Dominska, P. Greenwell, and T. D. Petes.** 1997. Microsatellite instability in yeast: dependence on repeat unit size and DNA mismatch repair genes. Mol. Cell. Biol. **17:**2851–2858.
49. **Sia, E. A., R. J. Kokoska, M. Dominska, P. Greenwell, and T. D. Petes.** 1998. Genetic control of microsatellite instability in *Saccharomyces cerevisiae*, p. 209–213. *In* R. H. Sarma and M. H. Sarma (ed.), Structure, motion, interaction and expression of biological macromolecules. Adenine Press, Albany, N.Y.
50. **Sikorski, R. S., and J. D. Boeke.** 1991. *In vitro* mutagenesis and plasmid shuffling: from cloned gene to mutant yeast, p. 302–318. *In* C. Guthrie and G. R. Fink (ed.), Guide to yeast genetics and molecular biology. Academic Press, San Diego, Calif.
51. **Strand, M., T. A. Prolla, R. M. Liskay, and T. D. Petes.** 1993. Destabilization of tracts of simple repetitive DNA in yeast by mutations affecting DNA mismatch repair. Nature **365:**274–276.
52. **Strand, M., M. C. Earley, G. F. Crouse, and T. D. Petes.** 1995. Mutations in the *MSH3* gene preferentially lead to deletions within tracts of simple repetitive DNA in *Saccharomyces cerevisiae*. Proc. Natl. Acad. Sci. USA **92:**10418–10421.
53. **Streisinger, G., Y. Okada, J. Emrich, J. Newton, A. Tsugita, E. Terzaghi, and M. Inouye.** 1966. Frameshift mutations and the genetic code. Cold Spring Harbor Symp. Quant. Biol. **31:**77–84.

54. **Tishkoff, D. X., N. Filosi, G. M. Gaida, and R. D. Kolodner.** 1997. A novel mutational avoidance mechanism dependent on *S. cerevisiae RAD27* is distinct from mismatch repair. Cell **88:**253–263.

55. **Tran, H. T., N. P. Degtyareva, N. N. Koloteva, A. Sugino, H. Masumoto, D. A. Gordenin, and M. A. Resnick.** 1995. Replication slippage between distant short repeats in *Saccharomyces cerevisiae* depends on the direction of replication and the *RAD50* and *RAD52* genes. Mol. Cell. Biol. **15:**5607–5617.

56. **Umar, A., A. B. Buermeyer, J. A. Simon, D. C. Thomas, A. B. Clark, R. M. Liskay, and T. A. Kunkel.** 1996. Requirement for PCNA in DNA mismatch repair at a step preceding DNA synthesis. Cell **87:**65–73.

57. **Wach, A., A. Brachat, R. Pohlmann, and P. Philippsen.** 1994. New heterologous modules for classical or PCR-based gene disruptions in *Saccharomyces cerevisiae*. Yeast **10:**1793–1808.

58. **Wang, T. S.-F.** 1996. Cellular DNA polymerases, p. 461–493. *In* M. L. DePamphilis (ed.), DNA replication in eukaryotic cells. Cold Spring Harbor Laboratory Press, Cold Spring Harbor, N.Y.

59. **Wickner, R. B.** 1994. [URE3] as an altered *URE2* protein: evidence for a prion analog in *Saccharomyces cerevisiae*. Science **264:**566–569.

60. **Wierdl, M., M. Dominska, and T. D. Petes.** 1997. Microsatellite instability in yeast: dependence on the length of the microsatellite. Genetics **146:**769–779.

61. **Zhang, P., J.-Y. Mo, A. Perez, A. Leon, L. Liu, N. Mazloum, H. Xu, and M. Y. W. T. Lee.** 1999. Direct interaction of proliferating cell nuclear antigen with p124 catalytic subunit of mammalian DNA polymerase δ. J. Biol. Chem. **274:**26647–26653.